Nonaxisymmetric Instabilities in a Dump Combustor with a Swirling Inlet Flow

M. Samimy*
Ohio State University, Columbus, Ohio
A. S. Nejad†
Aeropropulsion Laboratory, Wright-Patterson Air Force Base, Ohio
C. A. Langenfeld‡
Ohio State University, Columbus, Ohio
and
S. C. Favaloro§
Aeropropulsion Laboratory, Wright-Patterson Air Force Base, Ohio

A series of experiments was conducted to explore large-scale oscillations observed in a dump combustor with a swirling inlet flow. Inlets with different swirl profiles, namely constant angle, forced vortex, and free vortex, were used in these experiments. Three levels of swirl strength for the constant-angle swirl profile case and one swirl strength for the two other cases were tested. Well-organized large-scale oscillations were observed in all cases. Spatial correlation and phase measurements clearly identified different modes of nonaxisymmetric instabilities as the source of these energetic oscillations. The results also showed that swirl profile has as much effect as swirl strength on the combustor flowfield characteristics.

Nomenclature

D	= combustor diameter
f	= frequency
H	= step height
k,m	= axial and circumferential wave numbers
R	= radial coordinate
R_c	= combustor radius
R_f	= radius of forced-vortex portion of swirl velocity, Eq. (2)
R_h	= swirler hub radius
R_i	= inlet tube radius
S	= swirl number
SIG_U	= standard deviation of axial velocity
SIG_W	= standard deviation of tangential velocity
s	= slope of forced-vortex portion of swirl velocity, Eq. (2)
U,W	= mean axial and tangential velocities
U_{REF}	= inlet pipe centerline velocity
X	= axial coordinate
θ	= circumferential angle
θ_o	= incoming boundary-layer momentum thickness

Introduction

THE work presented herein is part of an ongoing research program to explore swirling flows in a dump combustor. Earlier, detailed two-component laser Doppler velocimetry (LDV) results were reported in an isothermal dump combustor with and without vortex breakdown.[1-3] Strong coherent oscillations were observed in both flows, especially for the case with no vortex breakdown. Additional exploratory research has been conducted to identify the nature of these oscillations. The results of this work are presented and discussed in this paper.

Received April 18, 1988; revision received Dec. 1, 1988.

*Assistant Professor. Member AIAA.
†Aerospace Engineer. Member AIAA.
‡Aerospace Engineer.
§Graduate Student.

Swirling flows have been the subject of extensive research efforts in a wide variety of engineering disciplines for many decades.[1-13] Large-scale oscillations in swirling flows have been observed and analyzed in detail by many researchers.[4-6] However, these types of flow oscillations have not been fully addressed in studies involving research combustors with swirling inlet flows. As will be detailed shortly, five swirl generators with curved inlet guide vanes were tested in the present experiments, and strong oscillations were observed in all five cases.

Experimental Facility and Instrumentation

Combustor Model

All the experiments were conducted in a cold-flow ramjet dump combustor model shown schematically in Fig. 1. The combustor model consisted of two major segments: the inlet assembly, and the combustor chamber and contraction nozzle section. The inlet assembly consisted of the following sections: a 300-mm-diam settling chamber; an inlet pipe, 2.85 m in length and 101.6 mm i.d.; and a cylindrical teflon swirl housing, 104.5-mm i.d., 152.4-mm o.d., 154 mm in length. The combustion chamber and contraction nozzle section consisted of a tube 1.85 m in length and 152.4-mm i.d. connected to a 30-deg converging nozzle with a 44% exit area ratio.

The unique feature of the research combustor was that the inlet assembly was supported on a traversing system controlled by a stepping motor. The entire inlet tube and the teflon swirler housing were capable of sliding through and traversing the length of the combustor chamber with a resolution of 0.025 mm. Two flat windows, 38×38 mm, were used for coincident two-component LDV measurements. One window was located on the inlet tube 94 mm upstream of the swirler, and the second window was located on the combustor wall 5.7 combustor diameters upstream of the contraction nozzle. The novelty of the system is that the aberration problems of two-component LDV associated with the curved wall of the combustor were eliminated, and at the same time the disturbances associated with the use of a flat window were kept to a minimum.

Five axial flow-type swirl generators were used in these experiments. Three of the swirl generators were of the con-

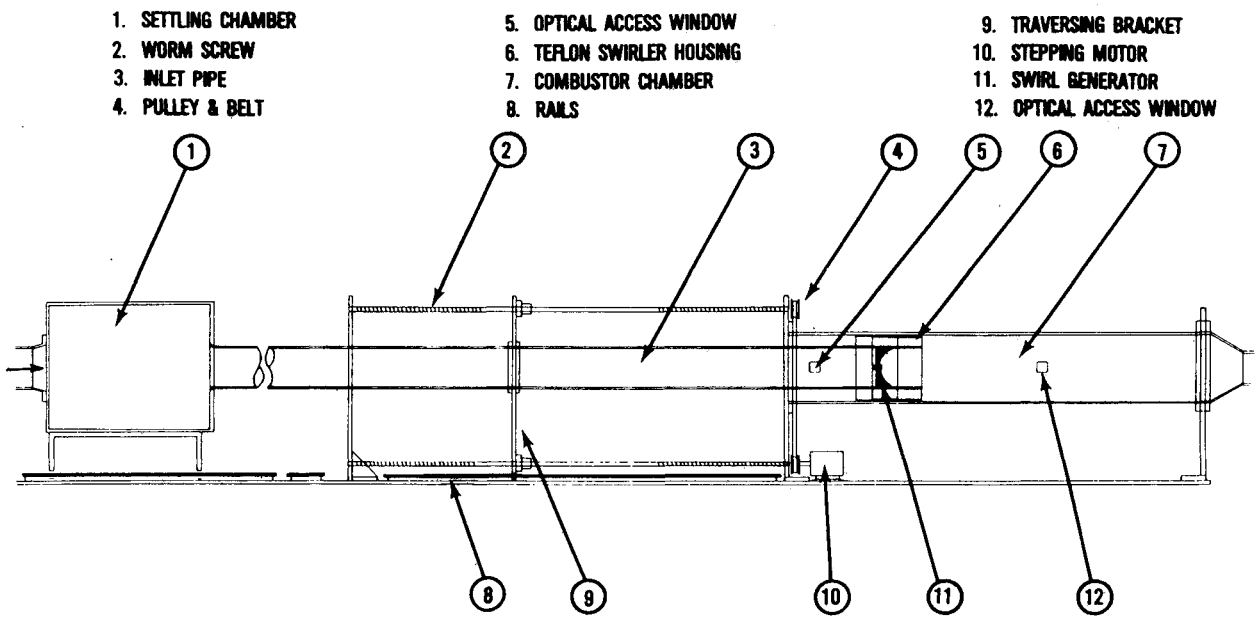

Fig. 1 Schematic of the experimental facility.

stant-angle type with swirl numbers of 0.3, 0.4, and 0.5, respectively. In addition, forced-vortex-type and free-vortex-type swirl generators with a swirl number of 0.4 were tested. The detailed design and construction of the swirl generators is described in Ref. 11. Each swirler had 12 curved inlet guide vanes welded between a 101.6-mm-i.d. outer ring and a 19-mm-o.d. central hub. The swirlers were located 50 mm upstream of the dump plane. Swirl numbers were determined based on the standard definition

$$S = \int_{R_h}^{R_1} UWr^2\,dr \Big/ \left(R_1 \int_{R_h}^{R_1} U^2 r\,dr \right) \qquad (1)$$

where U and W are the axial and tangential velocities and R_h and R_i are the hub and outer-ring radii.

Flow was induced by a centrifugal-type blower connected to the settling chamber by a flexible hose. The inlet centerline velocity was continuously monitored with a pitot probe located 266 mm upstream of the inlet pipe access window and was kept at 19.2 ± 0.4 m/s throughout these experiments, except where mentioned otherwise. The Reynolds number based on this velocity and the inlet tube diameter was approximately 125,000.

Instrumentation

A frequency-counter based, two-component coincident LDV system was used for velocity measurements. Titanium dioxide particles, smaller than 1μ in diameter, were used to seed the flow. The typical coincident data rate was 2000–6000/s with a 20-μs coincident window. The detail of the LDV system is given in Refs. 1–3.

Two TSI model 1210-T1.5 single-element hot-film probes were used for two-point correlation measurements. A Plantronics 4-mm-diam microphone located outside of the combustor chamber was used for obtaining acoustic signals. A model 660A Nicolet Scientific Corporation dual-channel FFT analyzer was used to obtain spectral densities of LDV, hot-film, and acoustic signals. Both the hot film and the acoustic signals were directly connected to the FFT analyzer. However, two different methods were utilized for the spectral analysis of LDV velocity fluctuations. In the first technique, a sample-hold fashion analog signal was obtained from the LDV frequency counter and analyzed using the FFT analyzer. In the second technique, the random digital data from LDV was sampled with a constant sampling rate of approximately 1/10 of the original data rate and used directly for power spectral analysis. In a preliminary comparison test, both methods gave similar results. Presently, necessary software for the second technique is in the developing stage. Therefore, only the results obtained using the first method will be presented here.

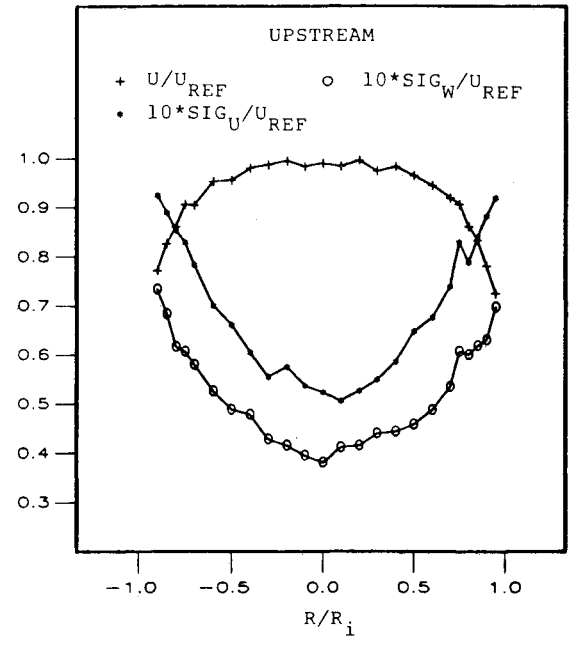

Fig. 2 Axial mean velocity and rms velocity fluctuations of inlet flow prior to swirl generator.

Experimental Results and Discussions

Mean Flow Results

As discussed earlier, the flat optical window located 94 mm upstream of the swirler housing was used for the incoming boundary-layer measurements. Figure 2 shows the mean axial velocity and the axial and tangential rms velocity fluctuations, normalized with respect to the inlet centerline velocity. The inlet centerline velocity was obtained using a pitot probe located 266 mm upstream of the inlet access window. The length of the inlet pipe from the settling chamber to the boundary-layer measurement location was approximately 2.8 m. This long tube generated a thick boundary layer with a momentum

thickness of approximately 2.9 mm. The turbulence intensity results are typical of fully developed turbulent pipe flow.

Figure 3 shows the significant effects of both swirl strength and swirl profile on the centerline velocity development. The effects of swirl strength in vortex flows have been investigated for decades.[4,5,8,11] Depending upon the Reynolds number and the strength of swirl, a phenomenon termed "vortex breakdown" may occur. Considering the constant-angle swirlers in the present experiments, for $S = 0.3$ and $S = 0.4$ flows, there is a large flow deceleration at the core of the vortex that is not strong enough to cause vortex breakdown. For $S = 0.5$ flow, vortex breakdown has occurred upstream of the dump plane, and the central recirculating flow has extended to approximately 4.2 step heights downstream of the step.

Comparison of the centerline axial velocity for different swirl profiles with the same swirl strength shows the significant impact of the swirl profile on the flowfield. While the $S = 0.4$ constant-angle and forced-vortex flows do not show any vortex breakdown, vortex breakdown has occurred with the free vortex, and the extent of the central recirculation zone is approximately 1.7 times larger than that of $S = 0.5$ constant-angle swirler. The swirl number, defined in Eq. (1), has been used to categorize the strength of swirl. Based on these results, it seems that the swirl number by itself is not a sufficient parameter to indicate swirl strength.

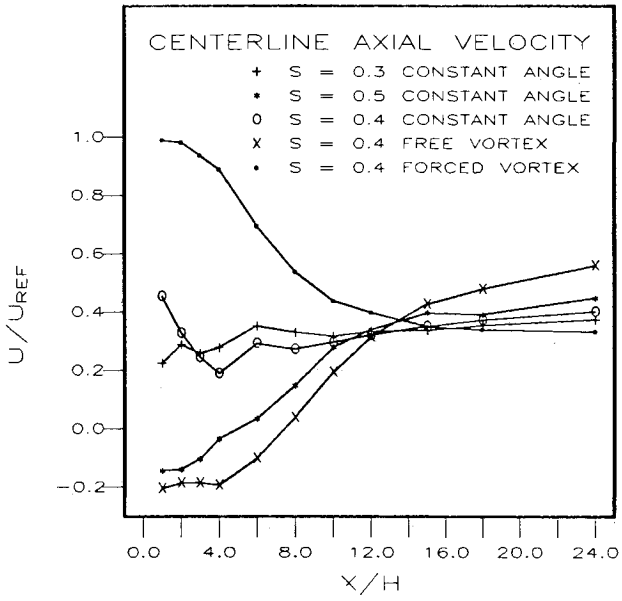

Fig. 3 Centerline axial velocity profiles for different swirl generators.

Figures 4 and 5 show radial distributions of mean axial and tangential velocities for all swirlers at two axial locations: two and six step heights from the dump plane. Four swirlers show similar axial velocity profiles with a significant axial momentum deficit in the central core. However, the forced vortex flow behaves like a jet flow and does not show any centerline axial momentum deficit. At a location of six step heights, the forced-vortex profile is almost like a forced vortex, the free vortex is like a Rankine vortex, but the constant-angle swirlers do not seem to belong to any known vortex category. Further downstream, the $S = 0.3$ flow turns into a forced vortex, and the $S = 0.5$ flow develops into a forced vortex at the center and a constant-velocity vortex outside of the central core.[1-3] Based on an inviscid stability analysis, Kurosaka[6,14] has shown that the second-order nonaxisymmetric disturbances tend to change the Rankine vortex profile of a Ranque-Hilsch tube into a forced-vortex-type profile; this matter will be discussed further.

Velocity Power Spectral Density Results

For all power spectral data, the digitization rate of the analog velocity signal was 2.56 times the expected maximum frequency in the flow. A low-pass filter with a cutoff frequency twice the expected maximum frequency was utilized. Power spectra were averaged over 50 blocks with each block containing 400 samples. For all the power spectral data reported here, the frequency resolution was less than 0.65 Hz, and the normalized standard error in amplitude was less than 15%.

Power spectral density analysis of the incoming boundary layer did not reveal any distinct frequencies. Detailed mean and turbulence results for the configuration with no swirl were presented in Refs. 1-3. The power spectral distributions for this configuration did not show any distinct frequencies in the free shear layer generated by the separation of the flow at the step. For free shear layers generated from an initial boundary layer with a uniform momentum thickness, such as the configuration with no swirl in the present experiments, linear stability theory[15] predicts the most amplified frequency to be $f = 0.017\ U_{REF}/\theta_o$, where U_{REF} and θ_o are the inlet velocity and momentum thickness, respectively. For the configuration with no swirl, this theory predicts a rollup frequency of approx-

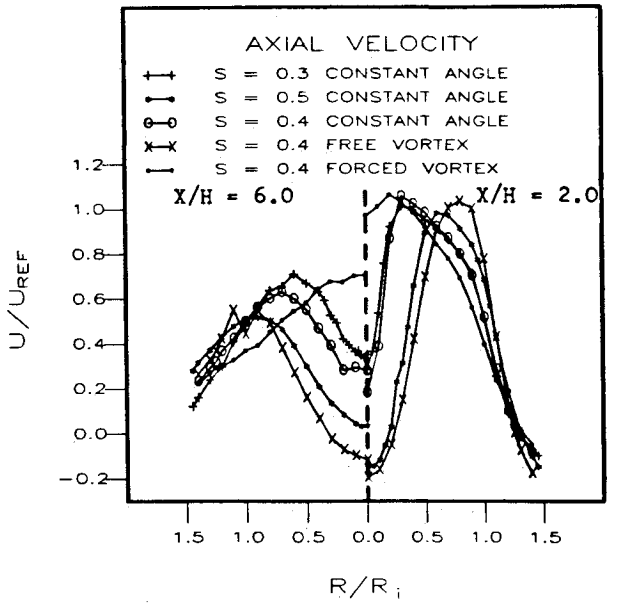

Fig. 4 Axial velocity profiles at $X/H = 2$ and 6.

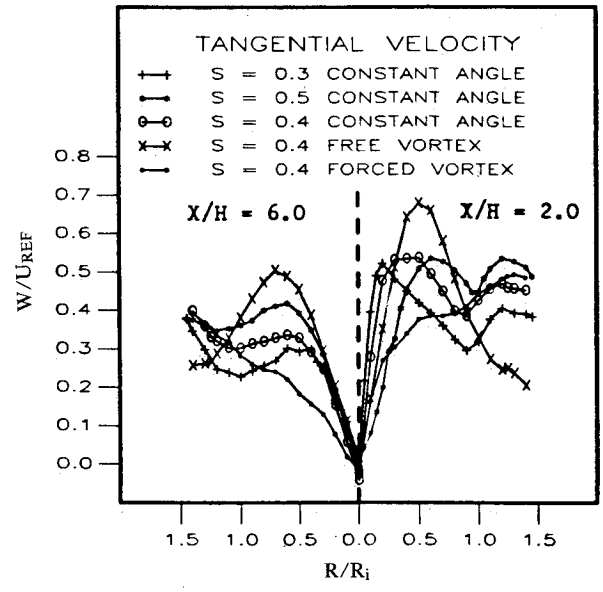

Fig. 5 Tangential velocity profiles at $X/H = 2$ and 6.

imately 110 Hz. In order to initiate the rollup of vortices in the experimental case, some sort of excitation, such as the longitudinal acoustic modes of the combustor chamber, is required. The range of the first acoustic mode of the present combustor, with the length of combustor varying from 0.87–1.48 m, is 120–200 Hz. Even with the longest combustor length, the first longitudinal acoustic mode is higher than the predicted rollup frequency of the shear layer. Apparently, there is no other source of excitation in the system or the laboratory environment with a frequency close enough to the most amplified frequency of the shear layer to provide external excitation.

As discussed earlier, each swirler had 12 curved inlet guide vanes welded between a 101.6-mm-i.d. outer ring and a 19-mm-o.d. central hub. The swirlers were located 50 mm upstream of the dump plane. With this arrangement, the initial boundary layer was destroyed while passing through the vanes. New boundary layers developed over the curved vanes. A wake developed behind the hub and a boundary layer developed inside the inlet pipe, after the swirler and before the separation at the dump plane. Thus, the flow downstream of the swirler is very complex, as reflected in Figs. 4 and 5.

Figure 6 shows power spectral density distributions of both axial and circumferential velocity fluctuations for the $S=0.3$ constant-angle swirler for different radial locations two step heights downstream of the dump plane. There are three peaks in the axial power spectra and two peaks in the tangential power spectra. These distinct peaks occur at approximately 5.5 Hz, 22 Hz, and 38 Hz, which seem to correspond to f, $4f$, and $7f$, f being the fundamental frequency. The peak is very sharp at f, relatively sharp at $4f$, and has a relatively large wideband at $7f$. The fundamental frequency appears at all radial locations, but $4f$ and $7f$ appear only in the shear layer generated from the expansion of the flow at the dump plane. Figure 7 shows the results for the same swirler at six step heights from the dump plane. The frequencies have not changed, but the energy level has decayed, except at 5.5 Hz in the tangential spectra.

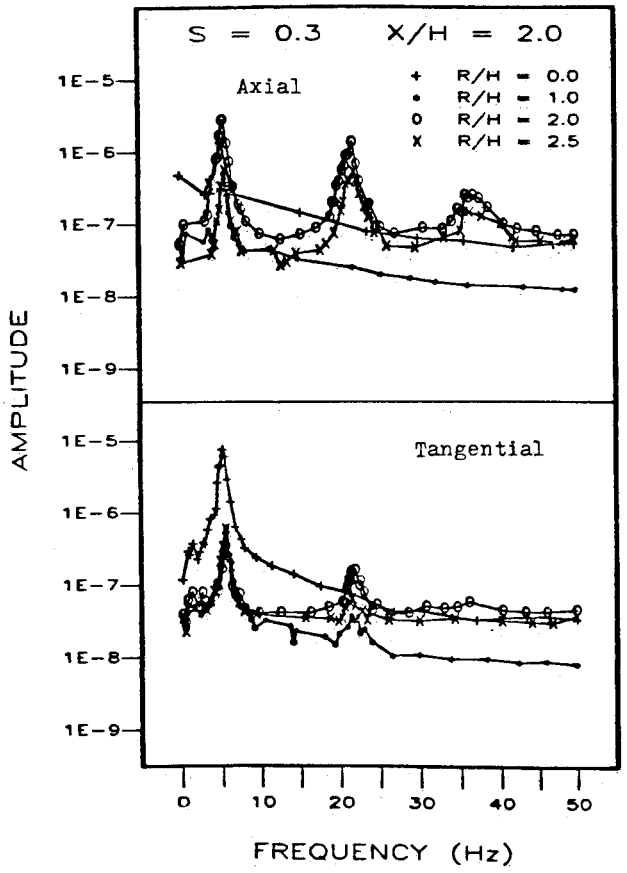

Fig. 6 Power spectral density distributions for $S=0.3$ at $X/H=2$.

For $S=0.4$ constant-angle and forced-vortex swirlers, the peak frequencies occurred at f, $3f$, and $5f$, where $f=8.5$ and 11 Hz for the constant-angle and the forced-vortex flows, respectively. Again, the peak at $5f$ was a wideband in both cases. Figure 8 shows the results for $S=0.5$ constant-angle

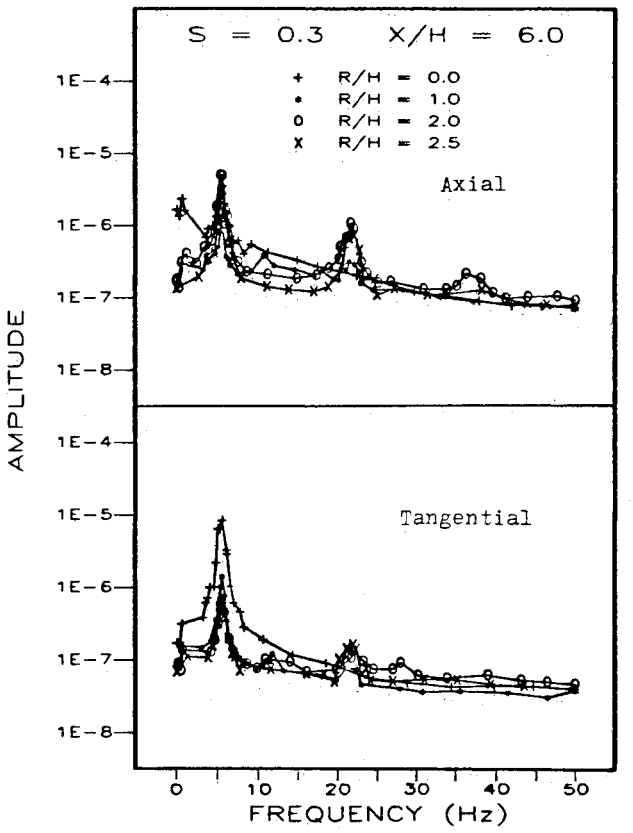

Fig. 7 Power spectral density distributions for $S=0.3$ at $X/H=6$.

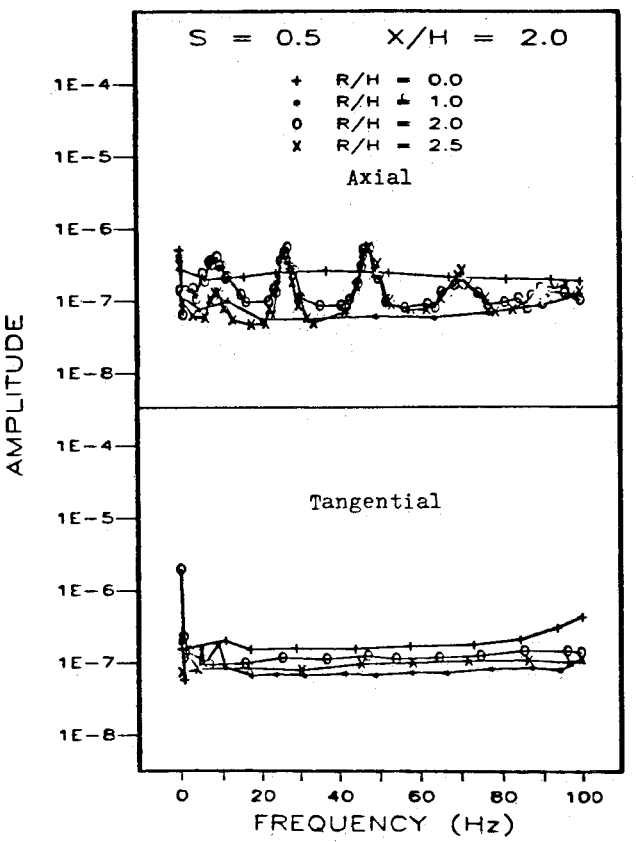

Fig. 8 Power spectral density distributions for $S=0.5$ at $X/H=2$.

swirler. Power spectra of axial velocity fluctuations show four peaks at 9, 27, 47, and 72 Hz, which appear to correspond to f, $3f$, $5f$, and $8f$. There was no distinct frequency inside the central recirculating zone. The energy level at the fundamental frequency is substantially less than that of $S = 0.3$ flow. Power spectra for the tangential velocity fluctuations do not show any distinct peaks. At six step heights downstream, $8f$ has disappeared and all the other peaks have significantly decayed.

While the power spectral results show some similarity among swirlers with different swirl number and profile, the results for $S = 0.4$ free vortex showed a totally different behavior, reconfirming that the swirl number is not the only parameter characterizing swirling flow behavior. At two step heights from the dump plane, the free-vortex flow showed either a single peak at approximately 98 Hz or two peaks, one at 98 and the other at 196 Hz. These frequencies appeared at the tangential velocity spectra at the centerline, at both velocity spectra at one step height radially from the centerline, and only at the axial velocity spectra at 2 and 2.5 step heights radially from the centerline. There was no distinct peak at six step heights axially from the dump plane.

A series of experiments was conducted with the $S = 0.3$ constant-angle swirler to determine the Reynolds-number dependency of the observed frequencies. Varying the Reynolds number based on the inlet tube centerline velocity and inlet tube diameter from 125,000 to 185,000, the Strouhal number based on the aforementioned velocity and diameter and the fundamental frequency was constant at 0.027. Also, $4f$ and $7f$ harmonics were observed in all cases.

Garg and Leibovich[5] have investigated the spectral characteristics of vortex breakdown flowfields in a tube with a small divergence angle. The Reynolds number (based on the tube diameter) in their experiments was almost an order of magnitude smaller than the Reynolds number in the present study. In the wake of vortex breakdown, they observed oscillations similar to those presented here, but with two major differences. First, they observed only the fundamental frequency and its first harmonic while selected harmonics were observed in the present experiments (Figs. 6 and 8). Second, their observed frequencies decreased in the streamwise direction. As an example, their fundamental frequency dropped from 13.3 to 4.7 Hz in one tube diameter in the streamwise direction. As can be seen from Figs. 6 and 7, there is no change in the frequencies in the streamwise direction in the present study.

Garg and Leibovich[5] used an inviscid linear stability analysis for parallel flows developed by Lessen et al.[16] and showed that these oscillations are associated with the normal mode of nonaxisymmetric instabilities in the flow. There are two major problems in applying Lessen's analysis to the present results. First, the axial profile used by Lessen et al. models either a jet-like or a wake-like profile. Figure 4 shows that the axial velocity profiles are neither type. Second, with a significant axial development in the flow, the flows in the present experiments cannot be characterized as parallel flows. Nevertheless, Lessen's analysis was used for $S = 0.3$ and 0.5 constant-angle swirlers. The results showed that $S = 0.3$ is stable and $S = 0.5$ is marginally stable to nonaxisymmetric disturbances. As was discussed, these flows did not satisfy two major requirements of Lessen's analysis. Thus, no conclusions can be drawn from these results.

In an isothermal dump combustor configuration with a Reynolds number comparable to that of the present experiments, Janjua and McLaughlin[10] observed oscillations with frequencies similar to those observed in the present experiments. They conducted only a limited number of experiments and did not show how these frequencies changed in the streamwise direction. They observed only the fundamental and the first harmonic, and these frequencies were insensitive to the radial location, which is consistent with present experiments. They showed that the Strouhal number, based on the inlet tube diameter and the maximum inlet velocity, was independent of the Reynolds number, which is also consistent with the present results discussed earlier. Their phase measurements indicated that the origin of the oscillations was nonaxisymmetric disturbances.

Vu and Gouldin[17] conducted research in isothermal confined coaxial swirling flows with Reynolds numbers comparable to those of the present experiments. They observed frequencies over an order of magnitude higher than the ones observed in the present experiments and the other experiments discussed.[5,10] Unfortunately, they did not give any details and did not offer any explanations for their results.

In order to further explore the nature of the observed oscillations, two single-wire hot-film anemometers were located two step heights from the dump plane and two step heights from the centerline of the combustor. Both hot films were oriented to measure the axial velocity fluctuations. The hot films were located either 90 or 180 deg apart in the circumferential direction. Cross-spectral densities were obtained for all five swirlers discussed. For nonaxisymmetric disturbances propagating on helical paths, the phase function is of the form $m\theta + kx - 2\pi$ ft. For given axial and radial locations and circumferential separation of the probes, one can determine the phase angle for various nonaxisymmetric modes m. For $m = 1,2,3$, and 4, the phase angle is determined to be 90, 180, -90, and 0 deg for 90-deg probe separation and 180, 0, 180, and 0 deg for 180-deg probe separation, respectively.

Figure 9 shows the cross-spectral density distribution and phase angle for the $S = 0.4$ forced-vortex case at 90-deg probes separation. There are three distinct peaks at approximately f,

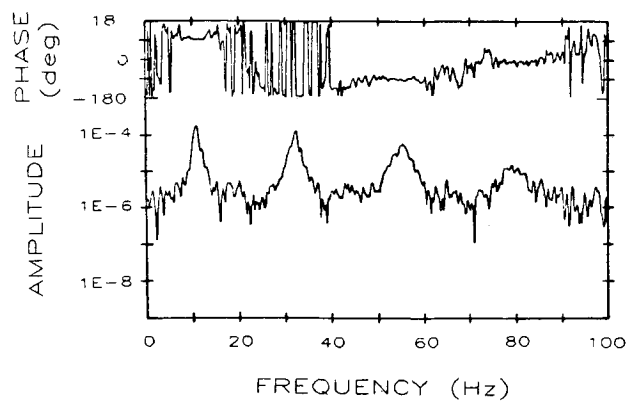

Fig. 9 Cross-spectral density and phase angle distributions for $S = 0.4$ forced vortex at $X/H = 2$ and 90-deg probe separation.

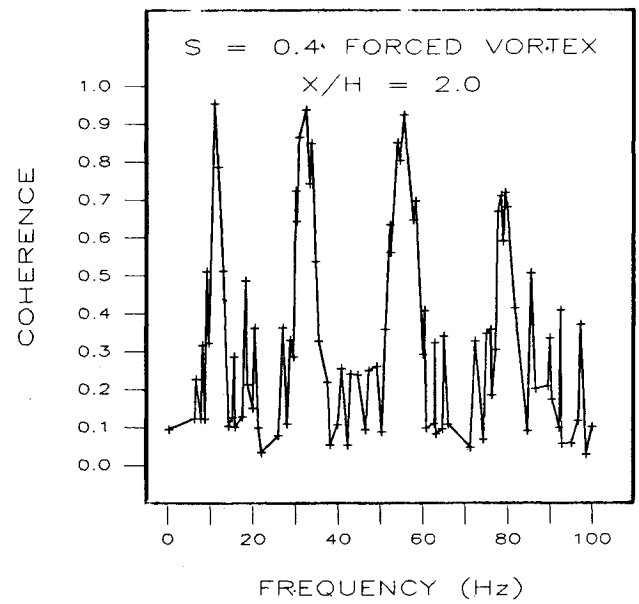

Fig. 10 Coherence function for conditions in Fig. 9.

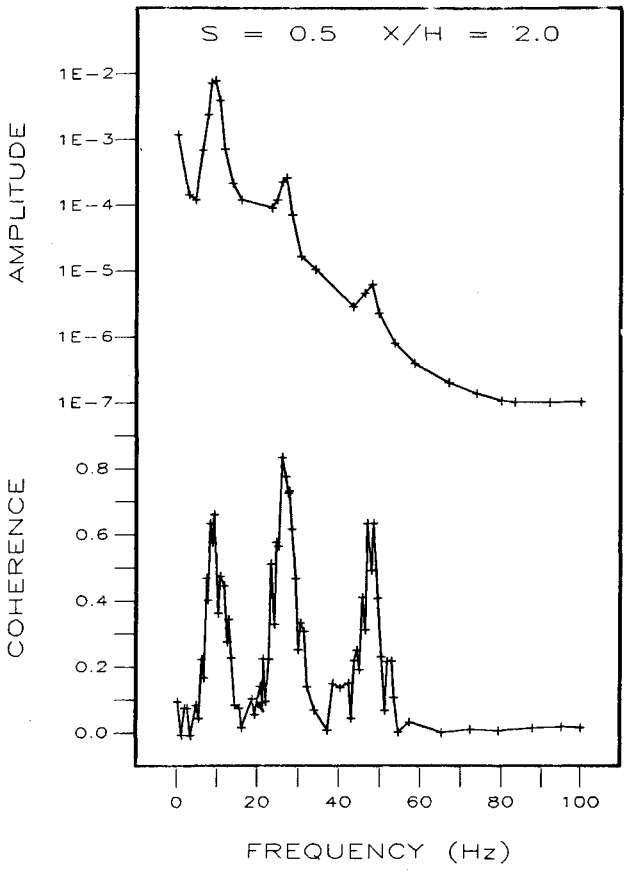

Fig. 11 Acoustic power spectral density and coherence function for acoustic velocity fluctuations.

$3f$, and $5f$ and one less distinct peak at $7f$, f being 11 Hz. As can be seen, the phase angles corresponding to these peaks are approximately 90, 180, −90, and 0 deg, which correspond to circumferential wave numbers of $m = 1,2,3$, and 4. The phase angles measured at 180-deg probes separation also confirmed these results. The results for all the other swirlers showed very similar behavior, confirming that one or more consecutive $m = 1,2,3,\ldots$ modes of nonaxisymmetric disturbances dominated the swirling dump combustor flows. Figure 10 shows the coherence function between the two mentioned signals and shows the coherence function to be almost unity for the first three modes and above 0.7 for the fourth mode. These results show extremely high coherent large-scale oscillations.

Acoustic Power Spectral Results

As discussed earlier, a 4-mm-diam microphone located outside of the combustor was utilized to obtain some information on the acoustic fields of the $S = 0.3$ and 0.5 constant-angle swirling flows. The microphone was located outside of the combustor approximately 10 mm from the combustor tube, perpendicular to the combustor axis, at either two or six step heights from the dump plane, the same axial locations shown in Figs. 4 and 5. Figure 11 shows the acoustic power spectrum at two step heights from the dump plane and the coherence function between the acoustic signal and the axial velocity signal obtained by LDV at the same axial location and 2.5 step heights radial location for the $S = 0.5$ constant-angle swirler. The spectrum shows peaks at the same frequencies as shown in Fig. 8, except for the peak at $8f$, f being 9 Hz. The coherence function shows values of 0.6, 0.84, and 0.6 at f, $3f$, and $5f$, respectively. The results at six step heights axial location were very similar to those of two step heights axial location.

The acoustic power spectra for $S = 0.3$ at two step heights axial location showed distinct frequencies at f and $4f$, f being 5.5 Hz. The coherence function between this acoustic signal and the axial velocity signal at the same axial location and 2.5 step heights from the centerline of the combustor were 0.6 and 0.5 at f and $4f$, respectively. The results at six step heights axial location were similar to those at two step heights axial location. It is important to note that the acoustic signals have been obtained in an open laboratory environment with fans, lasers, and many electronic devices operating. Therefore, the acoustic field generated by these nonaxisymmetric disturbances must be extremely strong to overcome all these background noises.

Table 1 Experimental and theoretical values of fundamental frequency, $m = 1$

Swirl no.	Swirl type	Location X/H	Experimental Hz	Theoretical Eq. (2), Hz
0.3	Constant	2	5.5	2.8
0.3	Constant	6	5.5	3.2
0.4	Constant	2	8.5	4.2
0.4	Constant	6	8.5	4.5
0.5	Constant	2	9.0	8.4
0.5	Constant	6	9.0	6.6
0.4	Forced	2	11.0	—
0.4	Forced	6	11.0	14.5
0.4	Free	2	98.0	9.0
0.4	Free	6	98.0	9.5

The Ranque-Hilsch effect in a vortex tube that generates separation in total temperature has been known for decades.[18] Recently, Kurosaka has explored the Ranque-Hilsch effect by a series of experimental and analytical studies.[6,14,19] He has shown that nonaxisymmetric disturbances are the source of vortex whistle, a pure tone heard in high Reynolds number swirling flows, which interact with and deform the mean flow and generate the total temperature separation. He showed that the vortex whistle deformed the mean flow profile from the Rankine vortex into a forced vortex. By suppressing the vortex whistle, both the Ranque-Hilsch effect and the velocity deformation disappeared. Kurosaka's inviscid instability analysis shows that for the Rankine-type velocity profile and for the positive circumferential wave numbers, the oscillating frequencies correspond to

$$f = s\,[m - 1 + (R_c/R_f)^{-2m}]/2\pi \qquad (2)$$

where m is the circumferential wave number, R_c is the combustor radius, R_f is the radius of the forced-vortex portion of swirl velocity, and s is the slope of this portion of the velocity profile.

As discussed earlier, the results of the present experiments identified circumferential wave numbers as $m = 1,2,3$, or 4. However, the profiles shown in the Fig. 5 do not have Rankine characteristics. Nevertheless, R_f and s obtained from the profiles of Fig. 5 were used in Eq. (2) to determine oscillation frequencies for different m values. Table 1 shows the fundamental frequencies observed in the present experiments and the frequencies obtained using Eq. (2). There is a reasonable agreement, except for the free-vortex case, between experimental and theoretical frequencies for this mode, but larger differences were observed for higher values of m. Kurosaka assumes that the flow is parallel. Figures 3–5 show a significant development in the flow that could explain the differences between the present experimental results and the results obtained using Eq. (2).

Conclusions

A detailed experimental investigation was carried out to determine the effects of inlet swirl profile on a dump combustor flowfield and the nature of coherent large-scale oscillations observed earlier in the flowfield. The results showed that the swirl profile has as much effect as the swirl number. The flowfields are dominated by extremely coherent, nonaxisymmetric oscillations. In most of the cases studied here, up to

four modes of oscillations corresponding to circumferential wave numbers of 1,2,3, and 4 were observed.

Acknowledgment

This research was supported by the U.S. Air Force Office of Scientific Research, monitored by Dr. Julian Tishkoff.

References

[1]Samimy, M., Nejad, A. S., and Langenfeld, C. A., Craig, R. R., and Vanka, S. P., "Isothermal Swirling Flow in a Dump Combustor," AIAA Paper 87-1352, June 1987.

[2]Samimy, M. and Langenfeld, C. A., "An Experimental Study of Isothermal Swirling Flows in a Dump Combustor," *AIAA Journal*, Vol. 26, Dec. 1988, pp. 1442-1449.

[3]Langenfeld, C. A., "A Study of Isothermal Swirling Flows in a Dump Combustor," M.S. Thesis, The Ohio State University, Columbus, OH, 1988.

[4]Leibovich, S., "Vortex Stability and Breakdown: Survey and Extension," *AIAA Journal*, Vol. 22, Sept. 1984, pp. 1192-1206.

[5]Garg, A. K. and Leibovich, S., "Spectral Characteristics of Vortex Breakdown Flowfields," *Physics of Fluids*, Vol. 22, Nov. 1979, pp. 2053-2064.

[6]Kurosaka, M., "Acoustic Streaming in Swirling Flow and the Ranque-Hilsch (Vortex-Tube) Effect," *Journal of Fluid Mechanics*, Vol. 124, 1982, pp. 139-172.

[7]Gouldin, F. C., Depsky, J. S., and Lee, S.-L., "Velocity Field Characteristics of Swirling Flow Combustor," *AIAA Journal*, Vol. 23, Jan. 1985, pp. 95-102.

[8]Lilley, D. G., "Swirling Flows in Typical Combustor Geometries," AIAA Paper 85-0184, Jan. 1985.

[9]Ramos, J. I. and Somer, H. T., "Swirling Flow in a Research Combustor," *AIAA Journal*, Vol. 23, Feb. 1985, pp. 241-248.

[10]Janjua, S. I. and McLaughlin, D. K., "An Experimental Study on Swirling Confined Jets with Helium Injection," Rept. DT-8562-01, Dynamics Technology, Inc., Torrance, CA, 1986.

[11]Buckley, P. L., Craig, R. R., Davis, D. L., and Schwartzkopf, K. G., "The Design and Combustion Performance of Practical Swirlers for Integral Rocket/Ramjet," *AIAA Journal*, Vol. 21, May 1983, pp. 753-740.

[12]Gupta, A. K., Lilley, D. G., and Syred, N., *Swirl Flows*, Abacus, Turnbridge Wells, England, 1984.

[13]Beer, J. M. and Chigier, N. A., *Combustion Aerodynamics*, Wiley, New York, 1972.

[14]Kurosaka, M., Chu, J. Q., and Goodman, J. R., "Ranque-Hilsch Effect Revisited: Temperature Separation Traced to Orderly Spinning Waves or 'Vortex Whistle'," AIAA Paper 82-0952, June 1982.

[15]Michalke, A., "On Spatially Growing Disturbances in an Inviscid Shear Layer," *Journal of Fluid Mechanics*, Vol. 23, 1965, pp. 521-544.

[16]Lessen, M., Singh, P. J., and Paillet, F., "The Stability of a Trailing Line Vortex. Part I. Inviscid Theory," *Journal of Fluid Mechanics*, Vol. 63, Part 4, 1974, pp. 753-763.

[17]Vu, B. T. and Gouldin, F. C., "Flow Measurements in a Model Swirl Combustor," *AIAA Journal*, Vol. 20, May 1982, pp. 642-651.

[18]Hilsch, R. "The Use of Expansion of Gases in a Centrifugal Field as Cooling Processes," *Review of Scientific Instrument*, Vol. 18, No. 2, 1947, pp. 108-113.

[19]Kurosaka, M., Goodman, J. R., and Kuroda, H., "An Interplay Between Acoustic Waves and Steady Vortical Flow," AIAA Paper 83-0740, April 1983.